

Random Forest Classifier Based Prediction of Rogue waves on Deep Oceans

Pujan Pokhrel
Canizaro Livingston Center for Gulf
Informatics
University of New Orleans
New Orleans, LA, United States
ppokhrel@uno.edu

Julian Simeonov
Naval Research Laboratory
Stennis Space Center
Mississippi, United States
julian.simeonov@nrlssc.navy.mil

Elias Ioup
Naval Research Laboratory
Stennis Space Center
Mississippi, United States
elias.ioup@nrlssc.navy.mil

Mahdi Abdelguerfi
Canizaro Livingston Center for Gulf
Informatics
University of New Orleans
New Orleans, LA, United States
mahdi@cs.uno.edu

Md Tamjidul Hoque[†]
Canizaro Livingston Center for Gulf
Informatics
University of New Orleans
New Orleans, LA, United States
thoque@uno.edu

[†]*To whom correspondence should be addressed*

Abstract

In this paper, we present a novel approach for the prediction of rogue waves in oceans using statistical machine learning methods. Since the ocean is composed of many wave systems, the change from a bimodal or multimodal directional distribution to unimodal one is taken as the warning criteria. Likewise, we explore various features that help in predicting rogue waves. The analysis of the results shows that the Spectral features are significant in predicting rogue waves. We find that nonlinear classifiers have better prediction accuracy than the linear ones. Finally, we propose a Random Forest Classifier based algorithm to predict rogue waves in oceanic conditions. The proposed algorithm has an Overall Accuracy of 89.57% to 91.81%, and the Balanced Accuracy varies between 79.41% to 89.03% depending on the forecast time window. Moreover, due to the model-free nature of the evaluation criteria and interdisciplinary characteristics of the approach, similar studies may be motivated in other nonlinear dispersive media, such as nonlinear optics, plasma, and solids, governed by similar equations, which will allow for the early detection of extreme waves.

1. INTRODUCTION

Rogue waves are classified as waves having a height more than 2.2 times the significant wave height (H_s) in the wave field [1]. Sometimes, they are studied using various nonlinear equations, which assume that wave energy gets focused on these events and generates nonlinearity. In this paper, rogue waves have been studied under the second assumption. Rogue waves are observed in hydrodynamics [1], optics [2], quantum mechanics [3], Bose-Einstein condensates [4], and finance [5]. They are mainly studied analytically using the spectral algorithms applying some deterministic equations like the nonlinear Schrodinger equation [6, 7]. Although rogue waves may be needed in fiber optics to satisfy certain energy levels and to locate the information using matched filtering, they are dangerous in oceans and present a danger to the safety of marine operations. Examples of these events include the sinking of Prestige [8], El Faro [9], and damage to the Draupner platform [10]. To prevent these accidents, an early detection system with precise emergence time of these events is needed.

There are various methods for the early detection of nonlinear waves. For example, spectral techniques can be used by measuring the super-continuum patterns in the Fourier spectra before the rogue waves form [11]. However, checking the Fourier spectra solely would fail to give any clue about the expected emergence point (or time) of a rogue wave in a chaotic wave field. Although various spectral methods have also been proposed to include the

time-dependent information about the waves [12, 13], the prediction time is only in the order of seconds. While such short time scales may be beneficial for saving lives in oceans, they are not enough for avoiding exposure to such events. Later, Birkholz *et. al.* [14] proposed a Grassberger-Procaccia nonlinear time series algorithm for the prediction of rogue waves and have slightly improved the time scale. Likewise, AD Cattrell [15] proposed that machine learning/statistical methods could be used to predict rogue waves using characteristic wave parameters.

To achieve the goal of forecasting rogue waves, it is necessary to develop statistics based computational approaches that can reliably and rapidly identify and forecast rogue waves in chaotic wave fields like the oceans. In contrast with the deterministic equations, such statistical methods can be employed for predicting a wide range of instabilities and can also help simulate the physics of the equations without computing a set of equations periodically. Some of the classical nonlinear evolution equations include nonlinear Schrodinger equation [6, 7, 16], Davey-Stewartson system [17, 18], Korteweg-de Vries equation [19], Kadomtsev-Petviashvili equation [20], Zakharov equation [21] and fully nonlinear potential systems [22]. However, such equations only describe a specific instability and using a set of equations every time to forecast rogue waves is not possible for a continental/planetary scale prediction. Since the ocean waves are often bimodal/multimodal due to the presence of many wave-systems, it is assumed that rogue waves are more likely to occur when the distribution turns unimodal. Afterwards, we used various statistical machine learning methods to forecast rogue waves [23-27].

2. POSSIBLE CAUSES OF ROGUE WAVES

Various methods for the formation of rogue waves have been explored in the literature. Some of them include (a) Linear Superposition, (b) Nonlinear effects, and (c) wind-wave interactions.

a) Linear Superposition and weakly nonlinear effects

The most widely used theory for describing statistics of the surface gravity waves is the Gaussian theory, which assumes that waves are a linear phenomenon. However, the theory fails to account for nonlinear effects [28-32]. Considering the waves are weakly nonlinear, various methods have been developed for the narrowband unidirectional case [6, 28, 30, 32-38]. A more general theory for second-order interactions of waves in the random directional sea was derived by Sharma and Dean [39], which in theory should be able to capture the effects of wave steepness, water depth and directional spreading with no approximations other than the truncation of the small

amplitude expansion to the second order. However, this model only attributes the abnormal events in the sea to the linear superposition of the waves in the oceans. It is important to note that at the second-order in Stokes expansion, the crests are sharper and higher while the troughs are flatter and lower; there is also a long wave set down (e.g., see [40]), which causes a decrease in the mean surface in regions of groups of high waves. Supported by in-situ measurements, Forristall [41] looked at the distribution of simulated second-order long-crested (i.e. unidirectional) and short-crested waves and verified the predictions of the second-order theory. Linear superposition of waves thus remains one of the most likely mechanisms behind the formation of rogue waves. **Figure (1)** and **Figure (2)** show the evolution of the spectra when superposition is taking place. In such cases, more than one waves with similar frequency components and small incidence angles can combine to form a large wave.

Three mechanisms have been proposed to explain how superposition occurs. First, the waves of different scales and frequencies propagate at different speeds. Likewise, waves of the same scale propagate with different speeds depending on their steepness. Since the ocean wave spectrum is continuous, all the waves within the spectrum are present and propagate at the same time in a random wave field [40]. Similarly, they can intersect and pile-up resulting in a higher surface elevation. Likewise, the wave fields with the same frequency and same steepness can be focused and superposed if they come from different angles [42]. This phenomenon is also known as wave focusing. While focusing is linear in this case, the last stage of the focused-wave dynamics demonstrates various nonlinear behaviors when the steepness is large enough [43]. Wave focusing due to directionality has been found to be a regular cause for wave breaking in wave tanks, which is associated with large waves [22]. If the waves of the same scale come from different directions, then a superposition of only two waves is needed to double wave height and steepness. These conditions can produce regular events with the height being the summation of two wave heights [44] or, at certain angles, activate some mechanisms of wave instability [45, 46]. Linear superposition of waves is most likely at small angles (which is not too dangerous) or at angles close to 180 degrees, which have been shown to be dangerous even at low significant wave heights [44]. Thus, linear superposition remains one of the most likely mechanisms behind the formation of large waves in the oceans.

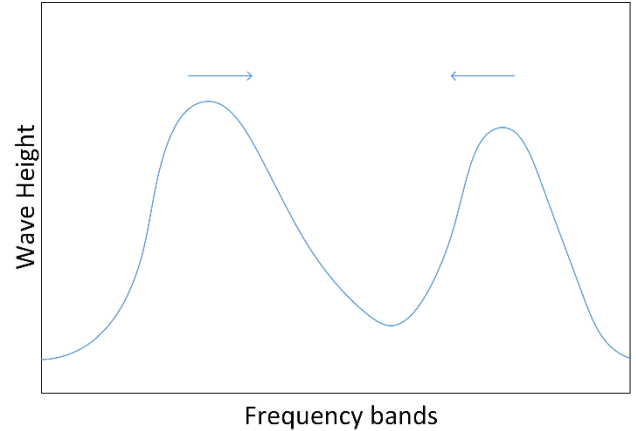


Figure 1: Example wave system with similar frequency components moving towards each other. Note that for superposition to occur, two waves have to move towards each other.

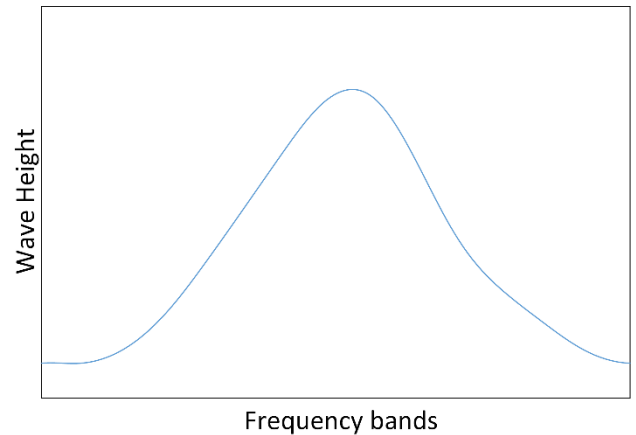


Figure 2: Superposition of two waves from Figure 1 to form a large wave. It shows how two waves traveling towards each other in Figure 1 can combine to form a large wave.

b) Nonlinear effects

A thorough description of different aspects of abnormal waves has been provided by Kharif et al. [1]. The authors present various possible causes behind rogue waves like wave focusing and higher-order nonlinearities. One of the most studied higher-order instability in wave systems is the Benjamin-Feir instability due to third-order quasi-resonant interactions between the free waves when the initial spectra represent narrowband long-crested conditions [46-49]. Higher-order models have also been explored, which point to the fact that large waves may be caused by various nonlinear effects in the ocean [6, 7, 16, 22, 36, 50-52]. The likelihood of this mechanism is quantified by the Benjamin-Feir Index (BFI) [53] (see also [54]). Favorable conditions

for the instability can be generated mechanically in wave tanks [55-58] or simulated numerically [49, 52, 54, 59, 60]. Miguel Onorato [55] provided the first experimental evidence that nonlinear wave statistics, mainly in the wave tanks and shallow water conditions, depend on BFI. Likewise, from the results of Petrova and Guedes Soares [38, 61-63], it is known that, in general, the wave nonlinearity increases with the distance from the wavemaker on experiments on the wave tank. Numerical studies [49, 57] analyzing the effect of the directionality show that the wave trains become increasingly unstable towards long-crested conditions. However, the initial requirements for the instability make this mechanism unlikely to be the primary cause for most extreme wave occurrences in oceanic conditions, characterized by the broader spectra and directional spread [41, 61]. It is important to note that the nonlinear statistics of the following sea states observed were usually lower than the mixed crossing seas with identical initial spectra. The results for the distribution of the wave heights corroborate the conclusion of Rodriguez [64] that the existence of two wave systems of different dominant frequencies but similar energy contents result in the reduction of probability of wave height higher than the mean and the effect becomes more significant as the intermodal distance increases. The higher-order wave nonlinearity is reported to increase significantly with the observed probability of occurrence of large wave events [59]. The third order wave-wave interactions expressed quantitatively by the mean of the coefficient of kurtosis, are considered in the case of Benjamin-Feir Instability, regarded as quasi-resonant four-wave interactions [48, 65]. It is observed that the high-frequency spectral counterpart for both following and crossing seas show a decrease in peak magnitude and downshift of the peak with the distance, as well as a reduction of spectral tail when modulational instability takes place [38, 47, 49]. The authors stress that that the results from removing the second and third-order bound wave effects from the nonlinear surface profiles show that, in some cases away from the wave generator, the wave parameters of the non-skewed profiles continue deviating largely from the linear predictions which justifies the need of using higher-order models for the description of wave data when free wave interactions become relevant. The result is well confirmed by a recent numerical experiment by Manolidis et al [66]. **Figure (3)** and **Figure (4)** show the evolution of the spectra when modulational instability and higher order nonlinear effects are taking place.

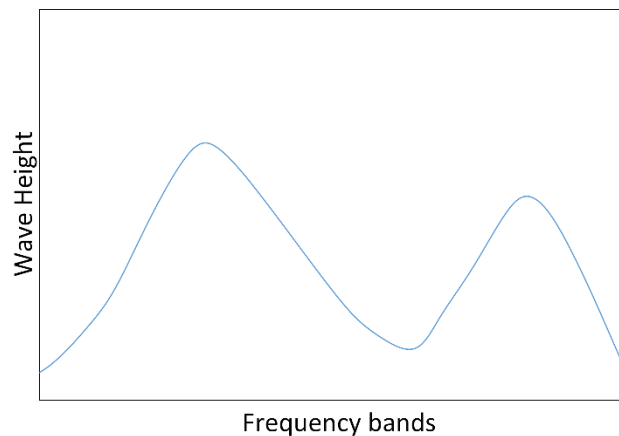


Figure 3: A directional distribution with two wave systems. The directionality of the waves is not essential for modulational instability.

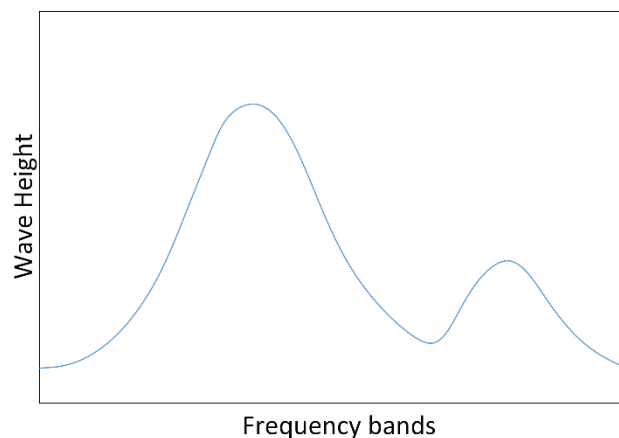


Figure 4: Example directional distribution when an extreme wave is occurring due to directional spreading. Note that as one wave undergoes the broadening of spectra, the other wave sucks up the energy from it to grow large.

c) Wind-wave interactions

It is known that storm waves are one of the five key processes identified in UKCP Marine Report that pose a great coastal risk in terms of flooding and inundation effects [67]. During storms, locally generated wind waves combine with the long period ocean swells to produce bimodal waves. Some reviews and comparisons of wave height distribution occurring after the storms in both deep and shallow water have been studied widely [30, 37, 41, 62, 68]. The analysis of the oceanic data collected in the stormy seas seems to indicate the validity of linear models for the distributions of large wave heights [30, 69, 70]. However, deviations between the theoretical predictions and observations occur at low probability levels when the measurements contain rare, huge waves, referred to as

abnormal, rogue or freak waves [38].

Likewise, interactions between oceanic swell and sea components can cause nonlinear interactions required for freak waves to occur. The effect of combined sea components on the wave crest statistics, surface elevation, skewness, and kurtosis were shown for the first time by Bitner-Gregersen and Hagen [71] for the second-order time-domain simulations. Higher wave crests and larger nonlinear statistics have been reported for wind-dominated seas. Arena and Guedes Soares [37] performed Monte Carlo simulations of the second-order waves with the bimodal spectra representative of the Atlantic Ocean. They reported good statistical agreements between the empirical wave height distributions and the linear model of Bocotti [72-74] and also between the distributions of nonlinear wave crests/troughs and second-order formulation of Fedele and Arena [35]. Petrova [38] presented the results of the contribution of the third-order nonlinearity to the wave statistics both in terms of angle of incidence between the two crossing wave systems and the evolution of the waves along with the tank. The authors also conclude that distributions of the wave crests and troughs for a large angle of crossing seas are more likely to be predicted by weakly nonlinear models rather than the linear ones.

In some studies, such as Burcharth, Hawkes *et al.*, Battjes, Reeve, [75-78] the phenomenon of wave bimodality has been elaborately described. Wind waves are characterized by one spectral peak with one significant wave height and one peak period. A bimodal (double-peaked) spectrum is usually formed through the combination of swell from a distant storm and locally generated wind sea. Transformations of these wave systems can be described in terms of wave crests, troughs and wave height distributions. Longuet-Higgins [79] proposed the Rayleigh distribution of wave heights and several modifications have been made to the low wave-height exceedance distributions [30, 62, 68, 72, 80-82]. Specifically, a depth modified version of the Rayleigh distribution was proposed by Battjes and Groenendijk [77] which is applied only to the unimodal waves. Similarly, Rodriguez [64] studied the wave height probability distributions using extracted gaussian bimodal waves from numerical simulations. The study classifies bimodal seas as wind-dominated, swell-dominated and mixed-sea conditions. Likewise, Petrova and Guedes Soares applied a linear quasi-deterministic theory to compare the energies from wind and swell seas using a simplified Sea-Swell energy ratio (SSER) on the assumption of wave nonlinearity [61]. Similarly, Norgaard and Lykke Anderson developed a slope dependent version of Rayleigh distribution based on an Ursell number criterion [83]. It should be noted that none of these studies have applied bimodal sea states that have varying proportions of swell,

while at the same time containing a fixed amount of energy to investigate wave height distribution in shallow/deep water close to a structure, which is what occurs very often in practice. However, the studies are sufficient to conclude that the interactions of various swell-sea and wind-sea components can lead to the formation of a large wave.

3. RELATED METHODS

To the best of our knowledge, there exist two works for prediction of rogue waves: (a) work by Will Cousins *et al.* [84, 85] and (b) work done at ECMWF by Janssen [86]. The work by Cousins *et al.* focuses on the short-term prediction of extreme events in irregular unidirectional fields. The algorithm can only predict 2-3 minutes into the future and needs high-resolution information from LIDAR about all neighboring waves to make predictions. Thus, it can't be used for prediction for a longer time period. It is also essential to note that the waves in the oceans are rarely unidirectional. They are mostly bidirectional or multidirectional. Moreover, only Benjamin-Feir instability analyzed in the paper using nonlinear Schrodinger and other nonlinear equations to predict rogue waves. In the ocean fields, where it is common to have a bidirectional wavefield with a swell-sea component, the initial requirements for Benjamin-Feir instability to occur might not occur. Likewise, Janssen [86] proposed a shallow water version of the Freak wave warning system. The system is based on an estimate of kurtosis and skewness proposed for a narrowband version of the theoretical expressions for skewness and kurtosis. However, their system is only applicable to the shallow waters and narrow banded wave trains.

Thus, in this paper, we propose a novel method to predict rogue waves in oceanic waters under broader conditions. The only assumption we make in this paper is that since the ocean is bimodal or multimodal when the distribution turns unimodal, freak waves are more likely to occur. However, we do not make any assumption on the initial conditions for the nonlinear phenomenon to occur. This model-free assumption allows us to capture various nonlinear effects without being restricted by a specific equation. Moreover, we take the time window for each sample to be 26.67 min which is somewhat stationary. Due to the model-free nature of our evaluation mechanism compared to other methods, we propose that it should be able to capture various nonlinearities in the oceanic wavefields.

4. DEVELOPMENT OF COMPUTATIONAL METHODS FOR FORECASTING ROGUE WAVES

4.1. Dataset

The historical dataset of the oceanic waves around the United States is collected via CDIP buoys and is available at the NOAA website. We used the data from January 2007 to October 2019 for the study. Due to the huge amount of data, we only retained 40% of the total data as the benchmark dataset for the study. There are 754490 positive points and 189345 negative points in the benchmark dataset. Please note that the data was shuffled before the training and the testing phases to avoid any bias arising due to data collection.

4.2. Feature selection for prediction of rogue waves

Many features have been used to identify rogue waves. The features used in this paper were derived from the Fourier spectra of the Directional Spreading Function after Discrete Fast Fourier Transform. It is important to note that the buoys don't always measure the same frequency components. It is thus necessary to derive the features that are adaptable to varying frequency components length. Likewise, these features also help to reduce the number of features significantly. The following features were derived from the four Fourier moments.

$$\sum_i^{n-1} \text{mean} \left(\sum_{j=i+1}^n \text{minowski}(X[:i], X[:j], k) \right) \quad (1)$$

$$\sum_i^{n-1} \text{mean}_c \left(\sum_{j=i+1}^n \text{mean}_c(X[i:j]) \right) \quad (2)$$

$$\sum_i^{n-1} \text{mean}_c \left(\sum_{j=i+1}^n \text{median}_c(X[i:j]) \right) \quad (3)$$

$$\sum_i^{n-1} \text{mean}_c \left(\sum_{j=i+1}^n \text{median}_c(X_R[i:j]) \right) \quad (4)$$

$$\sum_i^{n-1} \text{mean}_c \left(\sum_{j=i+1}^n \text{mean}_c(X_R[i:j]) \right) \quad (5)$$

$$\frac{1}{n} \sum \text{kurtosis} \quad (6)$$

$$\frac{1}{n} \sum \text{skewness} \quad (7)$$

$$\frac{1}{n} \sum \text{energy} \quad (8)$$

$$\frac{1}{n} \sum \text{direction} \quad (9)$$

where *mean_c* and *median_c* refer to column-wise mean and median respectively of the array derived from Fourier coefficients at different frequencies. Likewise, *X_R* refers to the array reversed in order, *minowski* refers to the Minowski distance function. It is used because it is the generalization of Euclidean and Manhattan distances. The values of *k* used are 0 and 1. The value of *i* and *j* vary from 0 to 27 and cover the frequency bands in the spectra from 0.025 Hz to 0.580 Hz. Here, in equation (1) we calculate the mean Minowski distances between various frequency components. Measuring the mean distance will help us measure the intermodal distances, which in turn, helps identify various nonlinear effects. Likewise, the other equations (2), (3), (4) and (5) capture the information about the general shape of the directional distribution. It is done by measuring the average mean and median which helps identify skewed distributions. The main intuition behind the features is that rogue waves occur due to various linear/nonlinear interactions between waves and thus measuring how the mean and median fluctuates between different frequency components interact should capture more information about the rogue waves. Moreover, it is to be noted that when modulational instability occurs, it is characterized by the spreading of the initial narrowband spectra. In such cases when the wave-wave interactions occur, it is common to observe that one wave system grows at the expense of another. Thus, these features should be helpful in identifying various nonlinearities in the oceans.

Equation (6) and Equation (7) define the normalized kurtosis and skewness of the wave directional distribution. The equations for calculating skewness and kurtosis are described in section 4.3. Specifically, equations (14) and (15) describe formula to calculate skewness and kurtosis respectively. Likewise, equation (8) refers to the normalized sum of energy and equation (9) refers to the normalized sum of directions of different frequency components of Fourier spectra.

The other features derived are significant wave height, peak frequency, peak bandwidth, peak direction, total energy of the system and the dominant wave period.

4.3. Distinguishing unimodal sea state from bimodal/multimodal sea state

To calculate the unimodal sea state, we calculate the kurtosis and skewness from the Discrete FFT derived from the time series data at each frequency band. The assumption is that when the energy gets focused, nonlinear effects occur

generating unimodal distribution and increasing likelihood for rogue waves to occur.

The estimate of the KVH criteria [87] is based on an integration over the frequency band 0.025 Hz to 0.580 Hz on the bulk Fourier moments a_1 , b_1 , a_2 , b_2 weighted by the energy density.

$$\begin{bmatrix} a_1 \\ b_1 \\ a_2 \\ b_2 \end{bmatrix} = \frac{1}{E^b} \int_{0.025}^{0.580} (df E(f)) \begin{bmatrix} a_1(f) \\ b_1(f) \\ a_2(f) \\ b_2(f) \end{bmatrix} \quad (10)$$

$$\begin{aligned} &\text{where } E^b \text{ is the variance with} \\ E^b &= \int_{0.025}^{0.580} df E(f) \end{aligned} \quad (11)$$

afterwards, we calculate

$$\theta = \tan^{-1}\left(\frac{b_1}{a_1}\right) \quad (12)$$

$$m_1 = (a_1^2 + b_1^2)^{1/2} \quad (13)$$

$$m_2 = a_2 * \cos(2 * \theta) + b_2 * \sin(2 * \theta) \quad (14)$$

$$n_2 = b_2 \cos(2\alpha) - a_2 \sin(2\alpha) \quad (15)$$

$$\text{skew} = \left(\frac{-n_2}{(1-m_2)}\right)^{3/2} \quad (16)$$

$$\text{kurtosis} = \frac{(6 - 8m_1 + 2m_2)^2}{2(1 - m_1)} \quad (17)$$

In equation (10), the bulk Fourier moments are derived to calculate the bulk KVH criteria. We take the integration of the Fourier moments multiplied by energy and bandwidth. It is then normalized by dividing it with variance calculate in equation (8). Likewise, equation (10) is used to calculate the bulk Fourier moments. Afterward, we use equation (12), (13) and (14) to find different parameters which are used to calculate skewness and kurtosis. Finally, we calculate the skewness and kurtosis in equation (16) and (17), respectively. Afterward, the KVH criteria are used to determine the unimodal distribution. KVH showed that the skewness and kurtosis are very sensitive to the secondary directional peaks and thus can be used to identify bimodal/multimodal distribution from a unimodal one. Although the KVH criteria are derived on the assumption of the unimodal distribution and describe the two peaked spectra as a warning criterion, we use the same criteria because of its model-free attributes but define the warning criteria as to when a unimodal distribution arises. The KVH criteria are given in the equations (18) and (19).

$$\text{kurtosis} < 2 + |\text{skew}| \text{ and } |\text{skew}| \leq 4 \quad (18)$$

$$\text{kurtosis} < 6 \text{ and } |\text{skew}| > 4 \quad (19)$$

5. RESULTS AND DISCUSSIONS

In this section, we present the results of the experiments that were carried out in this study. All the methods were implemented using python language. The Scikit-learn library [88] was used for implementing the machine learning algorithms. Note that 10 fold cross-validation was used for testing the classifiers. Please note that the window of 26.67 min corresponds to 1600s and is a standard for most NOAA buoys.

a) Performance of Logistic Regression with and without the spectra features

In this section, we compare the performance of the Logistic Regression classifier with and without the features (1) to (9). The classifier that didn't include the novel features contained significant wave height, peak frequency, peak bandwidth, the total energy of the system and the dominant wave period as features. Please note that the window of 26.67 min corresponds to 1600s and is a standard for most NOAA buoys.

Table 1: Performance of Logistic Regression with and without Spectral features

Methods	With	Without
Sensitivity	0.9125	0.7650
Specificity	0.7570	0.4520
Balanced Accuracy	0.8347	0.6085
Overall Accuracy	0.8663	0.4785
FPR	0.2429	0.5481
FNR	0.0874	0.2350
Precision	0.8988	0.1150
F1	0.9056	0.1990
MCC	0.6768	0.1220

Value in **bold** indicates the best outcome.

As we can see from **Table 1**, the performance of the Logistic Regression classifier increases when we use the spectral features proposed in equations (1) to (7). We thus take the features and test various machine learning algorithms to choose the best model. Note that the same

features have been used for predicting rogue waves for all the time windows.

b) Search for the best classifier for the time window 0-26.67 min

Table 2: Search for the best classifier for prediction

Methods	LogReg	KNN	RF	ET
Sensitivity	0.9125	0.9233	0.9474	0.9339
Specificity	0.7570	0.7259	0.8332	0.8405
Balanced Accuracy	0.8347	0.8246	0.8903	0.8872
Overall Accuracy	0.8663	0.8646	0.9135	0.9061
FPR	0.2429	0.2741	0.1667	0.1594
FNR	0.0874	0.0766	0.0526	0.0660
Precision	0.8988	0.8885	0.9308	0.9327
F1	0.9056	0.9055	0.9390	0.9333
MCC	0.6768	0.6685	0.7908	0.7751

LogReg=Logistic Regression, KNN=K Nearest Neighbors, RF=Random Forest, ET = Extra Tree

From **Table 2**, we can see that Random Forest performs the best with a Sensitivity of 0.9474, Specificity of 0.8332, Balanced Accuracy of 0.8903, Overall Accuracy of 0.9135, FPR of 0.1667, FNR of 0.0526, Precision of 0.9308, F1 0.9390 and MCC of 0.7908. The best parameters obtained for LogReg was C = 10, for KNN was 1300 trees. Similarly, the parameters obtained for Random Forest was max_depth=50, max_features=auto, min_samples_leaf=1, min_samples_split=2 and n_estimators=1000. Similarly, for ET, the best parameters were n_estimators=1500, and Bagging Classifier was built with 1000 trees and Decision Tree as the base classifier. Although Extra Tree performs better than the Random Forest Classifier on False Positive Rate and Specificity, we choose Random Forest Classifier because it performs best on all the other metrics.

c) Search for the best classifier for time window 26.67 min to 53.34 min

Table 3: Search for the best classifier for prediction

Methods	LogReg	KNN	RF	ET
Sensitivity	0.7755	0.9544	0.9621	0.9452
Specificity	0.7943	0.6369	0.6816	0.6957
Balanced Accuracy	0.7849	0.7956	0.8219	0.8205
Overall Accuracy	0.7796	0.8851	0.9009	0.8907
FPR	0.2056	0.3630	0.3183	0.3042
FNR	0.2244	0.0455	0.0378	0.3042

Precision	0.9310	0.9039	0.9154	0.9175
F1	0.8461	0.9285	0.9324	0.6947
MCC	0.49339	0.6434	0.6947	0.6687

LogReg=Logistic Regression, KNN=K Nearest Neighbors, RF=Random Forest, ET = Extra Tree

From **Table 3**, we can see that Random Forest performs the best with a Sensitivity of 0.9621, a specificity of 0.6816, Balanced Accuracy of 0.8219, Overall Accuracy of 0.9009, FPR of 0.3183, FNR of 0.0378, Precision of 0.9154, F1 of 0.9324, and MCC of 0.6947. Note that Logistic Regression has the highest Precision and Sensitivity among all the models tested and has the lowest False Positive Rate. However, we choose Random Forest Classifier because it beats all the other classifiers in other metrics. The best parameters obtained for LogReg was C = 1, for KNN was 1200 trees. Similarly, the parameters obtained for Random Forest was max_depth=40, max_features=auto, min_samples_leaf=2, min_samples_split=2 and n_estimators=800. Similarly, for ET, the best parameters were n_estimators=1000, and Bagging Classifier was built with 1000 trees and Decision Tree as the base classifier.

d) Search for the best classifier for time window 53.34 min to 80.01 min

Table 4: Search for the best classifier for prediction.

Methods	LogReg	KNN	RF	ET
Sensitivity	0.7699	0.9529	0.9591	0.9437
Specificity	0.7941	0.6144	0.6555	0.6614
Balanced Accuracy	0.7820	0.7837	0.8073	0.8020
Overall Accuracy	0.7750	0.8822	0.8957	0.8847
FPR	0.2058	0.3855	0.3444	0.3385
FNR	0.2300	0.0470	0.0408	0.0562
Precision	0.9340	0.9034	0.9133	0.9134
F1	0.8441	0.9275	0.9356	0.6664
MCC	0.4815	0.6206	0.6664	0.6366

LogReg=Logistic Regression, KNN=K Nearest Neighbors, RF=Random Forest, ET = Extra Tree

From **Table 4**, we can see that Random Forest performs the best with a Sensitivity of 0.9591, Specificity of 0.6555, Balanced Accuracy of 0.8073, Overall Accuracy of 0.8957, FPR of 0.3444, FNR of 0.0408, Precision of 0.9133, F1 of 0.9356, and MCC of 0.6664. We can see that Logistic Regression, however, has the highest Specificity and Precision and has the lowest False Positive Rate. However, it does not outperform Random Forest on all the other metrics. Thus, we choose Random Forest as the best

classifier. The best parameters obtained for LogReg was $C = 0.1$, for KNN was 1000 trees. Similarly, the parameters obtained for Random Forest was $\text{max_depth}=10$, $\text{max_features}=\text{'sqrt'}$, $\text{min_samples_leaf}=2$, $\text{min_samples_split}=2$ and $\text{n_estimators}=200$. Similarly, for ET, the best parameters were $\text{n_estimators}=1000$, and Bagging Classifier was built with 1000 trees and Decision Tree as the base classifier.

e) Searching for the best classifier for time window 80.01 min to 106.58 min

Table 5: Search for the best classifier for prediction

Methods	LogReg	KNN	RF	ET
Sensitivity	0.7657	0.9539	0.9699	0.9685
Specificity	0.7915	0.6093	0.6182	0.6203
Balanced Accuracy	0.7709	0.7816	0.7941	0.7944
Overall Accuracy	0.7709	0.8840	0.9181	0.9172
FPR	0.2084	0.3906	0.3817	0.3800
FNR	0.2343	0.0461	0.0300	0.0315
Precision	0.9352	0.9056	0.9363	0.9361
F1	0.8420	0.9291	0.9528	0.9522
MCC	0.4706	0.6172	0.6493	0.6462

LogReg=Logistic Regression, KNN=K Nearest Neighbors, RF=Random Forest, ET = Extra Tree

From **Table 5**, we can see that Random Forest performs the best with a Sensitivity of 0.9699. Specificity of 0.6182, Balanced Accuracy of 0.7941, Overall Accuracy of 0.9181, FPR of 0.3817, FNR of 0.0300, Precision of 0.9363, F1 0.9528 and MCC of 0.6493. We can see that Logistic Regression, however, has the highest Specificity and has the lowest False Positive Rate. However, it does not outperform Random Forest on all the other metrics. Thus, we choose Random Forest as the best classifier. The best parameters obtained for LogReg was $C = 1$, for KNN was 1300 trees. Similarly, the parameters obtained for Random Forest was $\text{max_depth}=20$, $\text{max_features}=\text{'sqrt'}$, $\text{min_samples_leaf}=2$, $\text{min_samples_split}=2$ and $\text{n_estimators}=400$. Similarly, for ET, the best parameters were $\text{n_estimators}=1000$, and Bagging Classifier was built with 1200 trees and Decision Tree as the base classifier.

We can see from the results that the performance of the classifiers increases when more features from the Fourier Spectra are included. Moreover, we can see that Logistic Regression, which is a weakly nonlinear model, can predict rogue waves from the normal waves with a considerable degree of accuracy. The results validate the conclusions of Petrova and Soares that weakly nonlinear models are still

helpful to predict nonlinear effects [38]. Moreover, the performance of the Tree-based methods like Random Forest and Extra Tree suggests that nonlinear models can capture various types of nonlinearity in the oceans. Likewise, since the Random Forest algorithm is very robust to noise compared to Extra Trees Classifier, it performs the best for all time windows explored in the paper. Moreover, as the prediction time for forecast increases, the Balanced Accuracy also decreases. It suggests that more features are required to forecast rogue waves for longer times.

6. CONCLUSIONS

From the results, we can conclude that it is possible to forecast rogue waves with the help of machine learning methods. First of all, we found that Spectral Features are important for forecasting rogue waves. Also, Random Forest outperforms all the other classifiers with Overall Accuracy and the Balanced Accuracy varying from 89.57% to 91.81%, and 79.41% to 89.03%, respectively, depending on the forecast time window.

With the use of model-free evaluation criteria, various Spectral Features, and statistical machine learning methods, the warning time for rogue waves has been improved from the scale of seconds/minutes to a scale of hours. We propose that a similar framework could be used to predict extreme events in other mediums, including but not limited to various nonlinear dispersive media.

REFERENCES

1. Christian Kharif, E.P., Alexey Slunyaev, *Rogue Waves in the Ocean*. Springer, 2009.
2. Zhengping Yang, W.-P.Z., Milivoj Belic, Yiqui Zhang, *Controllable optical rogue waves via nonlinearity management*. The Optical Society, 2018. **26**(6): p. 7587-7597.
3. Ni Song, Y.X., *Rogue Waves of Nonlinear Schrodinger Equation with Time-Dependent Linear Potential Function*. Discrete Dynamics in Nature and Society, 2016. **2016**.
4. Sitai Li, B.P., Gino Biondini, *Solitons and rogue waves in spinor Bose-Einstein condensates*. Physical Review E, 2018. **27**.
5. Yan, Z., *Financial Rogue Waves*. Communications on Theoretical Physics, 2009. **54**(5).
6. Boyd, J.P., *Nonlinear Wavepackets and Nonlinear Schroedinger Equation*. Dynamics of the Equatorial Ocean, 2017: p. 404-464.
7. Rabinowitz, P.H., *On a class of nonlinear Schrodinger equations*. Journal of Applied Mathematics and Physics, 1992. **43**(2): p. 270-291.

8. Cornelis Jan Camphuysen, M.H., Sherri Cox, Roberto Bao, D. Humple, C. Abraham, A. Sandoval, *The Prestige oil spill in Spain*. Atlantic Seabirds, 2002: p. 131-140.
9. Francesco Fedele, C.L., Arun Chawla, *The sinking of the El Faro: predicting real world rogue waves during Hurricane Joaquin*. Arxiv, 2017.
10. Mark McAllister, S.D., Thomas Adcock, Paul Taylor, Ton van den Bremer, *Laboratory recreation of the Daupner wave and the role of breaking in crossing seas*. Journal of Fluid Mechanics, 2019. **860**: p. 767-786.
11. B. Wetzel, A.S., L. Larger, P.A. Lacourt, J.M. Merolla, T. Sylvestre, A. Kudlinski, A. Mussot, G. Gentry, F. Dias, J.M. Dudley, *Real-time full bandwidth measurement of spectral noise in supercontinuum generation*. Scientific Reports, 2012. **2**(882).
12. Bayindir, C., *Compressive Spectral Method for the Simulation of the Nonlinear Gravity Waves*. Scientific Reports, 2016. **6**.
13. R.S. Gibson, C.S., *The evolution of large ocean waves: the role of local and rapid spectral changes*. Proceedings of the Royal Society A, 2006.
14. Simon Birkholz, C.B., Ayhan Demircan, Gunter Steinmeyer, *Predictability of Rogue Evens*. Physical Review Letters, 2015. **114**.
15. A.D. Cattrell, M.S., B.I. Moat, R. Marsh, *Can Rogue Waves Be Predicted Using Characteristic Wave parameters*. Journal of Geophysical Research: Oceans, 2018. **123**: p. 5624-5636.
16. Nail Akhmediev, A.A., J.M. Soto-Crespo, *Rogue waves and rational solutions of the nonlinear Schrodinger equation*. Physical Review E, 2009. **80**.
17. Felipe Linares, G.P., *On the Davey-Stewartson systems*. Annales de l'I.H.P. Analyse non lineaire, 1993. **10**(5): p. 523-548.
18. A. Davey, K.S., *On three-dimensional packets of surface waves*. Proceedings of the Royal Society A Mathematical, Physical and Engineering Sciences, 1974. **338**(1613).
19. Miura, R.M., *The Korteweg-de Vries Equation: A Survey of Results*. Society for Industrial and Applied Mathematics, 1976. **18**(3): p. 412-459.
20. B.B. Khadomtsev, V.I.P., *On the stability of solitary waves in weakly dispersive media*. Soviet Physics Doklady, 1970. **15**: p. 539-541.
21. Bidegaray, B., *On a nonlocal Zakharov equation*. Nonlinear Analysis: Theory, Methods and Applications, 1995. **25**(3): p. 247-278.
22. Dmitry Chalikov, A.V.B., *Three-Dimensional Periodic Fully Nonlinear Potential Waves*. International Conference on Offshore Mechanics and Arctic Engineering, 2013.
23. Aditi Kuchi, Md Tamjidul Hoque, Mahdi Abdelguerfi, Maik C. Flanagan, *Machine learning applications in detecting sand boils from images*. Array, 2019. **3-4**.
24. Avdesh Mishra, P.P., Md Tamjidul Hoque, *StackDPPred: A Stacking based Prediction of DNA-binding Protein from Sequence*. Oxford Bioinformatics, 2019. **35**(3).
25. Corey Maryan, Md Tamjidul Hoque, Christopher Michael, Elias Ioup, Mahdi Abdelguerfi, *Machine learning applications in detecting rip channels from images*. Applied Soft Computing, 2019. **78**: p. 84-93.
26. Sumaiya Iqbal, Md Tamjidul Hoque, *PBRpredict-Suite: a suite of models to predict peptide-recognition domain residues from protein sequence*. Oxford Bioinformatics, 2018. **34**(19): p. 3289-3299.
27. Suraj Gattani, A.M., Md Tamjidul Hoque, *StackCBPred: A stacking based prediction of protein-carbohydrate binding sites from sequence*. Carbohydrate Research, 2019. **486**.
28. Bourodimos, E.L., *Linear and nonlinear wave motion*. Reviews of Geophysics, 1968.
29. Harald E. Krogstad, O.A.A., *Linear Wave Theory*. Norwegian University of Science and Technology, 2000.
30. Mehmet Aziz Tayfun, F.F., *Wave height distributions and nonlinear effects*. Ocean Engineering, 2006. **34**(11-12).
31. Osborne, A.E., *Brief History and Overview of Nonlinear Water Waves*. International Geophysics, 2010. **97**: p. 3-31.
32. Osborne, A.R., *Nonlinear Fourier Analysis and Filtering of Ocean Waves*. International Geophysics, 2010. **97**: p. 713-744.
33. A.V. Gaponov, L.A.O., M.I. Rabinovich, *One-dimensional waves in disperse nonlinear systems*. Radiophysics and Quantum Electronics, 1970. **13**(2): p. 121-161.
34. S Hasselmann, K.H., J.H. Allender, T.P. Barnett, *Computations and parameterizations of the nonlinear energy transfer in a gravity-wave spectrum*. Journal of Fluid Mechanics, 1985. **15**.
35. Francesco Fedele, F.A., *Weakly nonlinear statistics of high random waves*. Physics of Fluids, 2005. **17**(2).
36. PK Shukla, I.K., B Eliasson, Mattis Marklund, *Instability and evolution of nonlinearly interacting water waves*. Physical Review Letters, 2006. **97**(9).
37. Felice Arena, C.G.S., *Nonlinear Crest, Trough, and Wave Height Distributions in Sea States With Double-Peaked Spectra*. Ocean Engineering, 2009. **131**(4).
38. Petya G Petrova, C.G.S., *Nonlinear probability distributions of waves in bimodal following and crossing seas generated in laboratory experiments*. Natural Hazards and Earth System Sciences, 2013.
39. J.N. Sharma, R.G.D., *Second-Order Directional Seas and Associated Wave Forces*. Society of Petroleum Engineers 1981. **21**(1).
40. Chen, X.B., *Set-down in the second-order Stokes' waves*. Proceedings of 6th International Conference on Hydrodynamics, Ischia (Italy), 2006: p. 179-185.
41. Forristall, G.Z., *Wave crests distribution: observations and second-order theory*. Journal of Physical Oceanography, 2000. **30**: p. 1931-1943.
42. Christophe Fochesato, S.G., Frederic Dias, *Numerical modeling of extreme rogue waves generated by directional energy focusing*. Wave Motion, 2007. **44**(5): p. 395-416.
43. Michael G. Brown, A.J., *Experiments on focusing unidirectional water waves*. Journal of Geophysical Research, 2001.
44. Greenslade, D., *A wave modelling study of the 1998 Sydney to Hobart yacht race*. Australian meteorological magazine, 2001. **50**: p. 53-63.
45. Alber, I.E., *The effects of randomness on the stability of two-dimensional surface wavetrains*. Proceedings of the Royal Society A, 1978.
46. Luigi Cavaleri, L.B., L. Torrisi, E. Bitner-Gregersen, M. Serio, M. Onorato, *Rogue waves in crossing seas: The Louis Majesty accident*. Journal of Geophysical Research, 2012.
47. Alessandro Toffoli, E.M.B.-G., A.R. Osborne, M. Serio, J. Monbaliu, Miguel Onorato, *Extreme waves in random*

- crossing seas: Laboratory experiments and numerical simulations.* Geophysical Research Letters, 2011.
48. Miguel Onorato, A.R.O., M. Serio, L. Cavaleri, C. Brandini, C.T. Stansberg, *Extreme waves, modulational instability and second order theory: wave flume experiments on irregular waves.* European Journal of Mechanics, 2006. **25**(5): p. 586-601.
 49. Miguel Onorato, L.C., O. Gramstad, P.A.E.M. Janssen, J. Monbaliu, A.R. Osborne. M. Serio. C.T. Stansberg, A. Toffoli, K. Trulsen, *Statistical properties of mechanically generated surface gravity waves: a laboratory experiment in 3D wave basin.* Journal of Fluid Mechanics, 2009. **627**: p. 235-257.
 50. Bayindir, C., *Compressive Spectral Method for the Simulation of the Nonlinear Gravity Waves.* Scientific Reports. **6**.
 51. Hasselmann, K., *On the non-linear energy transfer in a gravity wave spectrum. Part 2.* Journal of Fluid Mechanics, 1963. **15**.
 52. Nobuhito Mori, T.Y., *Effects of high-order nonlinear interactions on unidirectional wave train.* Ocean Engineering, 2002. **29**(10): p. 1233-1245.
 53. Janssen, P.A.E.M., *The Interaction of Ocean Waves and Wind.* Cambridge University Press, Cambridge, U.K., 2004.
 54. Miguel Onorato, A.R.O., M. Serio, S. Bertone, *Freak waves in random oceanic sea states.* Physical Review Letters, 2001. **86**: p. 5831-5834.
 55. Miguel Onorato, A.R.O., M. Serio, L. Cavaleri, C. Brandini, C.T. Stansberg, *Observation of strongly non-Gaussian statistics for random sea surface gravity waves in wave flume experiments.* Physical Review Letters, 2004. **70**.
 56. Takuji Waseda, T.K., Hitoshi Tamura, *Evolution of a Random Directional Wave and Freak Wave Occurrence.* Journal of Physical Oceanography, 2008.
 57. Hitoshi Tamura, T.W., Yasumasa Miyazawa, *Freakish sea state and swell-windsea coupling: Numerical study of the Suwa-Maru incident.* Geophysical Research Letters, 2009. **36**(1).
 58. Lev Shemer, A.S., *An experimental study of spatial evolution of statistical parameters in a unidirectional narrow-banded random wavefield.* Journal of Geophysical Research, 2009.
 59. Nobuhito Mori, P.A.E.M.J., *On Kurtosis and Occurrence Probability of Freak Waves.* Journal of Physical Oceanography, 2005.
 60. Herve Socquet-Jurglard, K.D., Karsten Trulsen, Harald E. Krogstad, Jingdong Liu, *Probability distributions of the surface gravity waves during spectral changes.* Journal of Fluid Mechanics, 2005. **542**.
 61. Petya G Petrova, C.G.S., *Wave height distribution in bimodal sea states from offshore basins.* Ocean Engineering, 2011. **38**(4): p. 658-672.
 62. Soares, C.G., *Representation of double-peaked sea wave spectra.* Ocean Engineering, 1984. **11**(2): p. 185-207.
 63. Soares, C.G., *On the occurrence of double peaked wave spectra.* Ocean Engineering, 1991. **18**(1-2): p. 167-171.
 64. German Rodriguez, C.G.S., Mercedes Pachenco, E. Perez-Martell, *Wave Height Distribution in Mixed Sea States.* Journal of Offshore Mechanics and Arctic Engineering, 2002. **124**(1): p. 34-40.
 65. Alessandro Toffoli, J.M.L., E. Bitner-Gregersen, J. Monbaliu, *Towards the identification of warning criteria: Analysis of ship accident database.* Applied Ocean Research, 2005. **27**: p. 281-291.
 66. Michail Manolidis, M.O., Julian Simenov, *Rogue Wave Formation in Adverse Ocean Current Gradients.* Journal of Marine Science and Engineering, 2019. **7**(2).
 67. Geoff J Jenkins, J.M.M., David M Sexton, Jason A Lowe, Phil Jones, Chris G Kilsby, *UK Climate Projections: Briefing Report.* Technical Report; Met Office Hadley Centre: Exeter, UK, 2010.
 68. Forristal, G., *On the Statistical Distribution of Wave Heights in a Storm.* Journal of Geophysical Research, 1978. **83**(C5): p. 2353-2358.
 69. Tayfun, M.A., *Distributions of envelope and phase in wind waves.* Journal of Physical Oceanography, 2008. **38**(12).
 70. Zhivelina Ivanova Cherna, M.A.T., Carlos Guedes Soares, *Statistics of nonlinear waves generated in on offshore wave basin.* Journal of Geophysical Research Atmospheres, 2009. **114**.
 71. E. Bitner-Gregersen, O.H., *Effects of two-peak spectra on wave crest statistics.* Proceedings of the 22nd International Conference on Offshore Mechanics and Arctic Engineering, 2003.
 72. Boccotti, P., *Wave Mechanics for Ocean Engineering.* Elsevier Science, 2000.
 73. Paolo Boccotti, *On Mechanics of Irregular Gravity Waves.* Atti della Accademia Nazionale dei Lincei, Memorie, 1989. **19**: p. 110-170.
 74. Paolo Boccotti, G.B., L. Mannino, *A field experiment on the mechanics of irregular gravity waves.* Journal of Fluid Mechanics, 1993. **252**: p. 172-186.
 75. Burcharth, H.F., *The effect of wave grouping on on-shore structures.* Coastal Engineering, 1978. **2**: p. 189-199.
 76. Peter J Hawkes, T.T.C., R J Jones, *Impacts of Bimodal Seas on Beaches and Control Structures.* Report, 1998.
 77. Jurgen A Battjes, H.W.G., *Wave height distributions on shallow foreshores.* Coastal Engineering, 2000. **40**(3): p. 161-182.
 78. Dominic E Reeve, A.J.C., *Coastal Engineering - Processes, Theory and Design Practice.* Spon. London, UK, 2012.
 79. Longuet-Higgins, M.S., *On the statistical distribution of height of sea waves.* Journal of Marine Research, 1952. **11**: p. 245-266.
 80. Tayfun, M.A., *Distribution of crest-to-trough waveheights.* Ocean Engineering, 1983. **10**(2): p. 97-106.
 81. Naess, A., *On the distribution of crest-to-trough waveheights.* Ocean Engineering, 1985. **12**(3): p. 221-234.
 82. Vinje, T., *The statistical distribution of waveheights in a random seaway.* Applied Ocean Research, 1989. **11**(3): p. 143-152.
 83. Jorgen Quvang Harck Norgaard, T.L.A., *Can the Rayleigh distribution be used to determine extreme wave heights in non-breaking swell conditions?* Coastal Engineering, 2016. **111**: p. 50-59.
 84. Will Cousins, M.O., Amin Chabchoub, Themistoklis P. Sapsis, *Predicting ocean rogue waves from point measurements: An experimental study for unidirectional waves.* Physical Review E, 2019.
 85. Will Cousins, T.P.S., *Reduced-order precursors of rare events in unidirectional nonlinear water waves.* Journal of Fluid Mechanics, 2016. **790**: p. 368-388.

86. Janssen, P.A.E.M., *Shallow-water version of the Freak Wave Warning System*, R. Department, Editor. 2017, ECMWF Technical Memoranda: England.
87. A.J. Kuik, G.P.v.V., L.H. Holthuijsen, *A Method for the Routine Analysis of Pitch-and-Roll Buoy Wave Data*. Journal of Physical Oceanography, 1988.
88. Pedregosa, F., et al., *Scikit-learn: Machine Learning in Python*. Journal of Machine Learning Research, 2011. **12**: p. 2825-2830.

Appendix

This section contains the definitions of the terminologies used in the text.

Linear Effect/ Nonlinear Effect: Gaussian Theory of waves assume that the waves can only interact with each other linearly. This is known as linear effects. However, recent experiments have shown that when waves combine, various nonlinear effects may take place. These effects can be studied with the help of nonlinear equations. So, they are also known as nonlinear waves

Stokes expansion: In fluid dynamics, a Stokes wave is a non-linear and periodic surface wave on an inviscid fluid layer of constant mean depth. This type of modelling has its origins in the mid-19th century when Sir George Stokes – using a perturbation series approach, now known as the Stokes expansion – obtained approximate solutions for non-linear wave motion

Steepness: The wave steepness is defined as the ratio of wave height H to the wavelength λ .

UKCP: United Kingdom Climate Projections

ECMWF: European Centre for Medium-Range Weather Forecasts

Pile up: accumulate

Wave instability: There are situations when a wave is capable of extracting energy from the system. It does so by drawing either kinetic energy from pre-existing motion or potential energy from background stratification. In either case the wave amplitude grows over time, and the wave is said to be unstable.

Nonlinear wave statistics: The statistics of the wave system when there are nonlinear waves present.

Modulational Instability: In the fields of nonlinear optics and fluid dynamics, modulational instability or sideband instability is a phenomenon whereby deviations from a periodic waveform are reinforced by nonlinearity, leading to the generation of spectral-sidebands and the eventual breakup of the waveform into a train of pulses. The phenomenon was first discovered – and modelled – for periodic surface gravity waves (Stokes waves) on deep water by T. Brooke Benjamin and Jim E. Feir, in 1967. Therefore, it is also known as the Benjamin–Feir instability.

CDIP: The Coastal Data Information Program (CDIP) specializes in wave measurement, swell modeling and forecasting, and the analysis of coastal environment data.

Directional Spreading Function: A directional wave spectrum can be described by $S(f, \theta) = S(f)D(\theta)$ where $S(f)$ is the energy density spectrum and $D(\theta)$ is the directional spreading function at frequency f . A general directional spreading function at frequency f can be expanded in angular Fourier series.

$$D(\theta) = \frac{1}{\pi} \left(\frac{1}{2} + \sum_{n=1}^{\infty} A_n \cos n\theta + B_n \sin n\theta \right)$$

Where A_n and B_n are the angular Fourier coefficients.

Fourier Moments: The moments derived from the function after Fourier transform. The first moment of a function $f(x)$ is given by

$$\int_{-\infty}^{\infty} x f(x) dx = \frac{-i}{2\pi} \frac{dF(0)}{ds}$$

Likewise, the n th moment is given by

$$\int_{-\infty}^{\infty} x^n f(x) dx = \left(\frac{-i}{2\pi} \right)^n \frac{d^n F(0)}{ds^n}$$

KVH criteria: The method proposed by A.J Kuik, G. Ph van Vledder and L.H. Holthuijsen for routine analysis of pitch-and-roll buoy data. It yields four directional model-free parameters per frequency to provide directional information: the mean direction, the directional width, the skewness, and the kurtosis of the directional energy distribution.

Minowski distance: Minowski distance is a generalized metric distance. When $\lambda = 1$, it becomes Euclidean distance. Similarly, Chebyshev distance is a special case of Minowski distance with $\lambda = \infty$. It can be used for both ordinal and quantitative variables. The formula is

$$d_{ij} = \sqrt[\lambda]{\sum_{k=1}^n |x_{ik} - x_{jk}|^\lambda}$$

Where d_{ij} refers to distance between two points and x_{ik} and x_{jk} refer to the coordinates of points i and j .